Korean J. Chem. Eng., **28**(10), 2081-2085 (2011)
DOI: 10.1007/s11814-011-0071-z

Biomimetic sequestration of carbon dioxide using an enzyme extracted from oyster shell

Dae-Hoon Kim*,, Mari Vinoba**, Woo-Sup Shin**, Kyong-Soo Lim**, Soon-Kwan Jeong**,†, and Sung-Hyun Kim*,†**

*Department of Chemical and Biological Engineering, Korea University, Anam-dong, Seongbuk-gu, Seoul 136-701, Korea
**Korea Institute of Energy Research, 71-2, Jang-dong, Yuseong-gu, Daejeon 305-343, Korea
(*Received 14 December 2010 • accepted 16 March 2011*)

Abstract−Carbon dioxide sequestration activity was compared and evaluated using bovine carbonic anhydrase (BCA), and a water soluble protein extract derived from hemocytes from diseased shell (HDS). *Para*-nitrophenyl acetate (p-NPA) was used to measure the reaction rate. The k_{cat}/K_m values obtained from the Lineweaver-Burk and Michaelis-Menten equations were 230.7 $M^{-1}s^{-1}$ for BCA and 194.1 $M^{-1}s^{-1}$ for HDS. Without a biocatalyst, $CaCO_3$ production took 15 seconds on average, while it took 5 seconds on average when BCA or HDS were present, indicating an approximately 3-fold enhancement of $CaCO_3$ production rate by the biocatalysts. The biocatalytic hydration of CO_2 and its precipitation as $CaCO_3$ in the presence of biocatalysts were investigated.

Key words: Carbon Dioxide, Sequestration, Bovine Carbonic Anhydrase, Hemocytes from Diseased Shell, Biomineralization

INTRODUCTION

Since the industrial revolution, fossil fuel consumption has drastically increased. Carbon dioxide discharged from combustion processes is now believed responsible for global warming and an increase in the earth's average temperature [1]. The carbon dioxide concentration in the atmosphere has increased by about 35% over the past 100 years, and it continues to increase by more than 0.4% each year, resulting in elevation of the sea level, abnormal air temperatures, and worldwide destruction of the ecosystem. The concentration of atmospheric greenhouse gases responsible for global warming, converted to carbon dioxide equivalents, is approximately 450 ppm. The actual carbon dioxide concentration is about 380 ppm, indicating that this gas accounts for more than 84% of the total greenhouse gases [2]. If the carbon dioxide discharge from fossil fuel combustion is not controlled, the carbon dioxide concentration in the atmosphere will continue to increase [3].

To reduce the emission of carbon dioxide, the greatest contributor to greenhouse effects among the six major greenhouse gases listed by the IPCC (Intergovernmental Panel on Climate Change), substantial efforts need to be aimed at increasing energy efficiency, use of nuclear power, the introduction of new and renewable energy sources, and the installation of CCS (carbon dioxide capture and storage) process. In the case of CCS, the ETP (Energy Technology Perspectives) report of the IEA (International Energy Agency) predicted that CCS processes will account for 19-22% of the carbon dioxide emission reduction by 2050 [4], indicating a significant role for CCS in reducing global warming.

The types of CCS technology that can be applied to mass carbon dioxide emitting processes, such as coal-fired power plant, can be divided into pre-combustion, post-combustion, and oxy-fuel combustion processes, with applied technologies that include absorption [5,6], adsorption [7,8], and membrane separation [9]. Among these methods, the absorption process is the most actively studied process, since it can conveniently capture large masses of carbon dioxide. However, the absorption process has some drawbacks such as erosion of the reaction apparatus by the applied solvent, loss of solvent due to volatility, and the need for high heat duty for regeneration of the solvent in stripper [10,11]. CCS also requires additional space for storage of the captured carbon dioxide. Currently, CCS is very expensive to install and to operate, resulting in a potential doubling of electricity costs. For this reason, many research programs are aimed at developing more economical CCS processes.

One of new technologies that can replace conventional CCS processes is carbon dioxide sequestration using a biocatalyst. Carbon dioxide capture by biocatalysts has a number of advantages, such as rapid carbon dioxide absorption, low energy requirements, no need for additional storage, and economic payback in the form of useful minerals following addition of an appropriate cation. Atmospheric carbon dioxide is dissolved in water through the following Eqs. (1) to (4) and, in the presence of an appropriate cation, precipitated minerals can be obtained, as shown in Eq. (5):

$$CO_{2(g)} \leftrightarrow CO_{2(aq)} \quad \text{Dissolution} \quad (1)$$

$$CO_{2(aq)} + H_2O \xleftrightarrow{k_2-k_{-2}} H_2CO_3 \quad \text{Carbonic acid reaction} \quad (2)$$

$$H_2CO_3 \xleftrightarrow{k_3-k_{-3}} H^+ + HCO_3^- \quad \text{Bicarbonate reaction} \quad (3)$$

$$HCO_3^- \leftrightarrow H^+ + CO_3^{2-} \quad \text{Carbonate reaction} \quad (4)$$

$$Ca^{2+} + CO_3^{2-} \rightarrow CaCO_3 \downarrow \quad \text{Calcium carbonate formation} \quad (5)$$

The rate k_2 of the carbonic acid reaction in Eq. (2) is 6.2×10^{-2} s^{-1} and k_{-2} is 23.7 s^{-1}, giving an equilibrium constant of 6×10^{-3}. In Eq. (3), the k_3 for the bicarbonate-forming reaction is 8×10^6 s^{-1} and the k_{-3} is 4.7×10^{10} s^{-1}, for an equilibrium constant of 1.7×10^{-4}, indicating that this reaction is a very fast, diffusion-controlled step. Therefore, the carbonic acid-forming step of Eq. (2) is the rate-determining

†To whom correspondence should be addressed.
E-mail: jeongsk@kier.re.kr, kimsh@korea.ac.kr
‡This work was presented at the 8th Korea-China Workshop on Clean Energy Technology held at Daejeon, Nov. 24-27, 2010.

step of the overall reaction [12,13]. Bicarbonate formed by Eq. (3) is easily converted to carbonate ion, which, in the presence of Ca^{2+} cations, can be readily precipitated in the form of calcium carbonate [14].

Carbonic anhydrase, which catalyzes the formation of bicarbonate from carbon dioxide, is a naturally occurring enzyme found in both animals and plants. Depending on its source, this enzyme has different properties, protein structure, molecular weight, and affinity for carbon dioxide. The human carbonic anhydrase II can hydrate 1.6×10^6 carbon dioxide molecules per second [15]. When carbonic anhydrase is employed for carbon dioxide hydration, the reaction goes through the following Eqs. (6) to (8). Carbonic anhydrase first forms OH^- through anhydrization. The carbon contained in carbon dioxide then carries out a nucleophilic attack on the Zn-bound OH and forms bicarbonate, which is then released by substitution with a water molecule.

$$E\bullet ZnH_2O \leftrightarrow EZnOH^- + H^+ \quad \text{Activation} \quad (6)$$

$$E\bullet ZnOH^- + CO_2 \leftrightarrow EZnHCO_3^- \quad \text{Association} \quad (7)$$

$$E\bullet ZnHCO_3^- + H_2O \leftrightarrow EZnH_2O + HCO_3^- \quad \text{Hydration} \quad (8)$$

The overall reaction is rapid because, in this new reaction pathway, the bicarbonate formed completely bypasses the rate-limiting step shown in Eq. (2).

Many studies have explored the use of biocatalysts for the capture and conversion of carbon dioxide, but most have relied on catalysts such as bovine carbonic anhydrase (BCA) and human carbonic anhydrase (HCA) [16]. Since it is difficult to extract these biocatalysts and replicate their genes, a new type of biocatalyst needs to be developed.

We studied carbon dioxide sequestration using hemocytes from diseased shell (HDS) and extra pallial fluid (EPF) extracted from oysters (*Crassostrea Gigas*) that are widely distributed in the sea. Carbon dioxide sequestration was studied by varying the conditions of HDS and EPF and comparing their effectiveness to that of BCA. We also investigated the kinetics of the biocatalyst reaction using para-nitrophenyl acetate (p-NPA) and followed biomineralization using calcium ions.

EXPERIMENTAL SECTION

1. Hydration of CO_2

The biocatalysts employed for the hydration of CO_2 and mineralization in this study were BCA, HCA (Sigma-Aldrich Co.), HDS, and EPF. Table 1 shows the molecular weight of the individual biocatalysts measured by MALDI-TOF: BCA 29 kDa, HCA 25.5 kDa, HDS 22.7 kDa and EPF 22.8 kDa. In the case of HDS and EPF, the molecular weight is difficult to measure since they are conjugated proteins. However, the analysis results in our study can be regarded as reliable because Lee et al. reported molecular weights measured by electrophoretic patterns as 22 kDa [17]. 0.1 M Tris-HCl buffer (Sigma-Aldrich Co.) solution was used to maintain pH 7.0 for the biocatalytic activity test. Biocatalyst catalyzes the hydration of CO_2, and consequently, hydrogen ions are transferred between the active site of the biocatalyst and the surrounding buffer solution. This results in a change in pH. The pH variation over time was monitored in real-time with a pH meter (Thermo Scientific Co. Orion Star Series). The experiment was carried out as a batch reaction. The desired reaction temperature was maintained by water circulating pump. Typically, 500 ml of 0.1 M Tris-HCl buffer was stirred at 150 rpm to enhance diffusion. Nitrogen was injected uniformly into the bottom of the reactor through a porous sintered metal plate to eliminate all residual gas-phase substances in the Tris-HCl buffer. The selected biocatalyst was then added and dissolved by stirring for 15 minutes. A mixture of carbon dioxide, oxygen, and nitrogen was then injected at a rate of 500 cc/min. Progress of the reaction was monitored by measuring pH of the mixture. The experiment was stopped when there was no further change in pH. Carbon dioxide concentration was mainly set at 12%, which is the average concentration in flue gas from a coal-fired power plant. Carbon dioxide concentration was also varied to 1% and 5% in the experiment. To determine the effect of temperature on the biocatalysts, we varied the temperature to 5, 25, and 60 °C and analyzed the hydration of CO_2.

Table 1. Molecular weight of biocatalysts by MALD-TOF analysis

Biocatalyst	kDa
BCA	29.0
HCA	25.5
HDS	22.7
EPF	22.8

2. Biocatalytic Assay by Hydrolysis of p-NPA

The biocatalytic activities of the biocatalysts were estimated spectrophotometrically using p-NPA as a substrate, as reported previous paper [18].

3. Biomineralization of CO_2

$CaCO_3$ precipitation was carried out after hydration of CO_2 in a batch reactor. To obtain the final product, $CaCO_3$, a saturated carbon dioxide solution was prepared. 500 ml of distilled water was stirred in the reactor at 150 rpm and 25 °C, while carbon dioxide was injected into it for three hours. $CaCl_2$ (Sigma-Aldrich Co.) was prepared as 0.1 M solution and the selected biocatalyst was dissolved into these solutions by mixing for 30 minutes. Then, a 20 ml sample of the previously prepared carbon dioxide solution was added to the mixture and stirred for formation of $CaCO_3$. The amount of $CaCO_3$ was determined after filtration and drying. After weighing of $CaCO_3$, the particle size and morphology of particles was measured by SEM, and the structure of the $CaCO_3$ was analyzed by XRD.

RESULTS AND DISCUSSION

1. Hydration of CO_2 by Biocatalyst

During the hydration of carbon dioxide with the biocatalysts, the pH decreases because hydrogen ions are released into the solution as the reaction $CO_2(g) \rightarrow CO_{2(aq)} \rightarrow H_2CO_3 \rightarrow HCO_3^- + H^+ \rightarrow CO_3^{2-} + H^+$ progresses. Fig. 1 shows the results of the hydration reaction at 5 °C with each of the biocatalysts. The pH dropped appreciably in the presence of the biocatalysts when compared with the pH change in the blank test. The pH drop was the fastest for BCA, indicating it to have the best efficiency for CO_2 hydration. The overall hydration rate was in the order of BCA>HDS>HCA>EPF. BCA and HDS, the biocatalyst that showed excellent hydration efficiency,

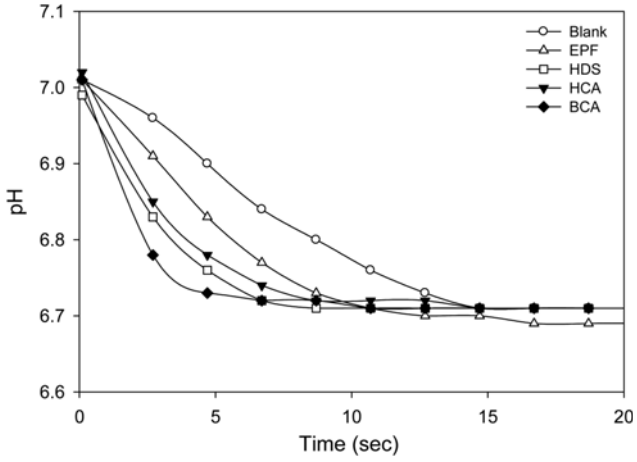

Fig. 1. Hydration of CO_2 with different biocatalysts.

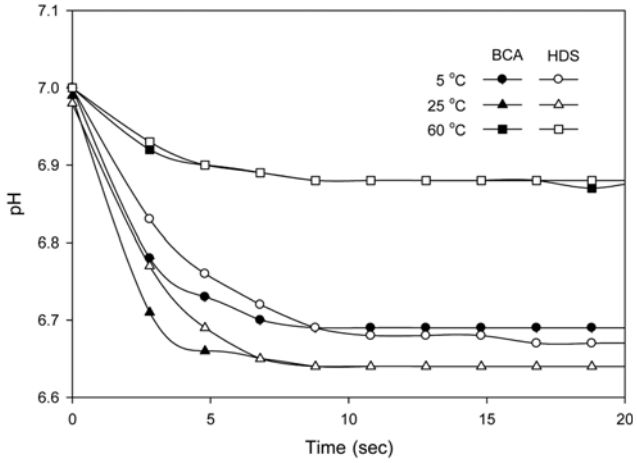

Fig. 2. Effect of temperature on hydration of CO_2 with BCA and HDS.

were selected for subsequent tests and the results were compared by varying the reaction temperature to 5, 25 and 60 °C, as shown in Fig. 2. The best activity was found at 25 °C for both BCA and HDS. This result is consistent with the result of Parissa et al.; the relative activity of BCA decreased with increasing temperature due to conformational changes that led to the unfolding of the protein of BCA [19]. It is well known that the biocatalytic activity is affected on the deformation of β-structure of the secondary structure of biocatalysts. The fraction of the β-structures in BCA and HDS is 36.8% and 20.5%, respectively. Thus, the activity of BCA would be expected to be more substantially reduced by temperature increases; however, the actual results were similar. The reason for this might be that HDS is a conjugated protein.

Fig. 3 shows the hydration of CO_2 characteristics of BCA and HDS in response to varied carbon dioxide concentration (1, 5, and 12%). Hydration of CO_2 was observed at all concentrations, indicating that the biocatalysts are capable of handling levels of carbon dioxide generated by some industrial processes and coal-fired power plants. In addition, these biocatalysts can maintain a stable CCS because they are not sensitive to sudden variations in carbon dioxide concentration, as their activity was maintained at various con-

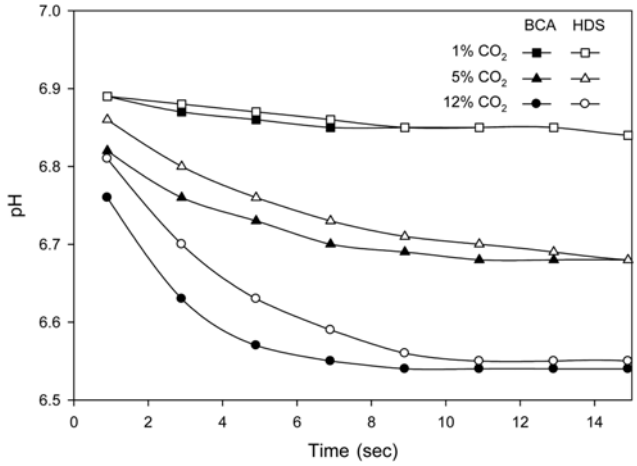

Fig. 3. Effect of CO_2 concentration on hydration of CO_2.

Table 2. Summary of the kinetic parameters of p-NPA hydrolysis by BCA and HDS

Enzyme	BCA	HDS
Eo (mmol/*l*)	0.18276	0.05
$1/V_{max}$	0.0213	0.61297
Slope	0.3953	1.71735
V_{max} (μmol/min)	46.9484	1.63151
K_m (mM)	18.5587	2.80187
k_{cat} (S^{-1})	4.2814	0.543836
k_{cat}/K_m ($M^{-1}S^{-1}$)	230.7	194.1

centrations. Therefore, they show potential for application in various areas of carbon dioxide sequestration in the future.

2. Hydrolysis of p-NPA Kinetics

The biocatalysts produce p-NP and acetic acid through an acyl-enzyme intermediate in the hydration reaction with p-NPA. The reaction pathway of p-NPA and CO_2 hydration for metalloenzymes is almost the same. Therefore, we can estimate the CO_2 hydration efficiency of metalloenzymes from the results of p-NPA hydrolysis. The K_m and k_{cat} values were obtained by the Michaelis-Menten (Eq. (9)) and Lineweaver-Burk (Eq. (10)) equations, and were used to calculate the rate constant, k_{cat}/K_m:

$$V = \frac{k_{cat}[S][Eo]}{K_m + [S]} \tag{9}$$

$$\frac{1}{V} = \frac{1}{V_{max}} + \frac{K_m}{V_{max}}\frac{1}{[S]} \tag{10}$$

where V is the rate of p-NP formation, V_{max} is the maximum rate, k_{cat} is the catalytic rate constant, $[E_0]$ the enzyme concentration, [S] is the p-NPA concentration, and K_m is the rate constant when the rate is equal to $V_{max}/2$, and k_{cat}/K_m is the kinetic constant.

The carbon dioxide reaction rate of BCA and HDS, measured through the p-NPA reaction, was determined by the absorbance, which is proportional to the reaction rate of BCA and HDS. The reaction rate of BCA was higher than that of HDS. Here, HDS is not a pure enzyme, as it consisted of several proteins. The reaction rates of HDS and BCA were similar at biocatalyst concentrations

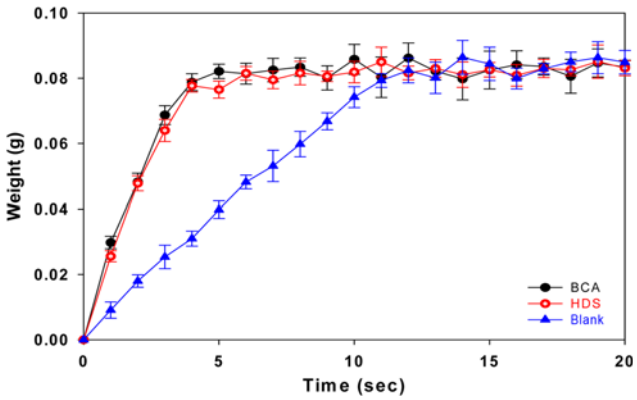

Fig. 4. $CaCO_3$ formation with or without biocatalyst.

above 1 μM. Table 2 summarizes all of the kinetic parameters. The k_{cat}/K_m rate constant was 230.7 $M^{-1}s^{-1}$ for BCA and 194.1 $M^{-1}s^{-1}$ for HDS. Considering that HDS is a water-soluble, conjugated protein, the k_{cat}/K_m value of HDS may be regarded as similar to that of BCA. This means that BCA, which is expensive and difficult to extract, can be replaced by the more economical HDS biocatalyst extracted from oysters.

3. Formation of $CaCO_3$

$CaCO_3$ was formed by adding Ca^{2+} ion to the CO_2 hydrated solution containing CO_3^{2-}. The amount of $CaCO_3$ was also measured at different times during the reaction. As shown in Fig. 4, the initial formation of $CaCO_3$ required about 15 seconds in the $CaCO_3$ precipitation experiment without the biocatalysts. In contrast, when

Table 3. Summary of precipitated calcium carbonate

	BCA		HDS	
	With	Without	With	Without
Structure	Calcite	Calcite	Calcite	Calcite
Weight of precipitate (g)	0.087	0.085	0.092	0.088
Rate of precipitate (sec)	4.93	15.15	5.21	15.16

BCA and HDS were added, $CaCO_3$ formation occurred within five seconds, on average, for a three-times faster formation rate. The final quantity of the produced $CaCO_3$ was the same since it was strongly dependent on the amount of CO_3^{2-} originally dissolved in the water. Table 3 summarizes the results of the precipitation of calcium carbonate.

Fig. 5 shows the size of the produced $CaCO_3$ analyzed by SEM. $CaCO_3$ particles produced without the biocatalysts were larger than 10 μm in diameter, but were less than 4 μm when BCA and HDS were used. There are two models that can describe size enlargement in precipitation system. One is the deposition of ionic or molecular species on crystal surfaces and the other is aggregation mode. The latter process is found to be the most important parameter to increase particle size. The aggregation mode depends on hydrodynamic conditions like agitation. In this study there is the same experimental condition; therefore, we can conclude that the particle size partially depends on the existence of enzyme. Berman et al. reported that a soluble protein, extracted from the shell of a mollusk, inhibited the particle growth [20]. However, in this study, the particle size with enzyme is smaller than that without enzyme. Additional study may

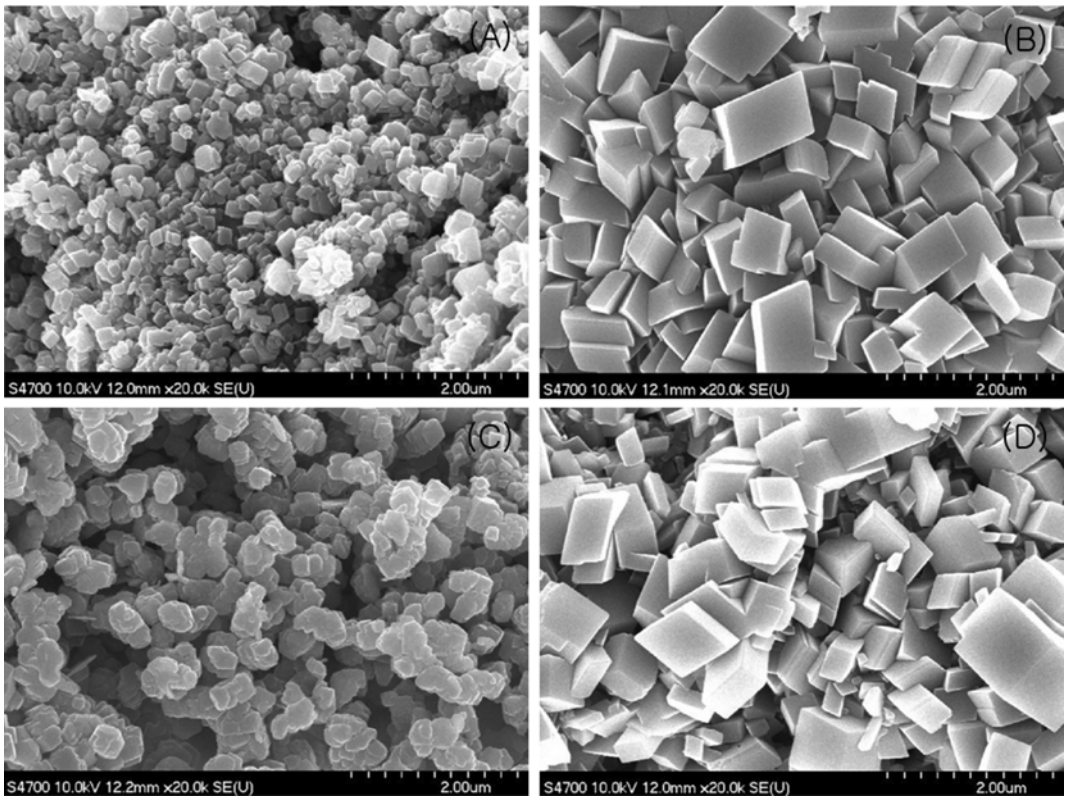

Fig. 5. SEM images of CaCO3 by (A) BCA (B) without BCA, (C) HDS, (D) without HDS.

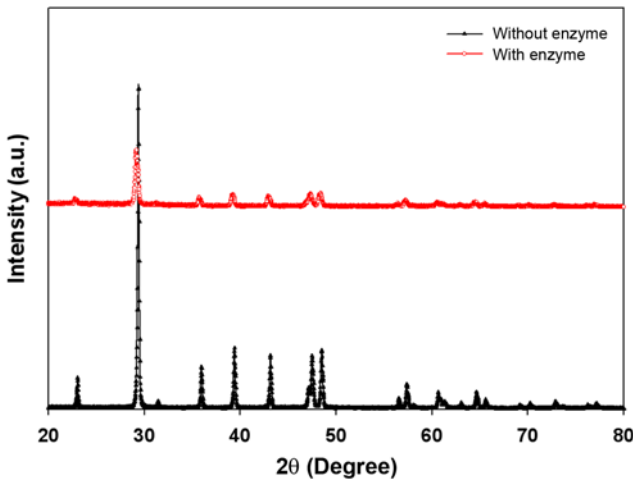

Fig. 6. XRD patterns of $CaCO_3$ precipitated by with or without biocatalyst.

be required in this regard.

A previous study mentioned that the $CaCO_3$ structure can be altered by the use of biocatalysts and that the reaction rate of hydration and mineralization can be determined by varying the concentration of the biocatalysts [21]. In addition, they reported that the $CaCO_3$ was a calcite structure, as shown by the calcite peak with 2θ=29° in the XRD analysis [18,20]. Fig. 6 shows the XRD results for the structure of the $CaCO_3$ produced in this study. The $CaCO_3$ structure may also be the calcite structure, as indicated by a calcite peak with 2θ=29°. The calcite structure was apparent with or without biocatalysts, indicating that the use of the biocatalysts did not effect the $CaCO_3$ structure of the reaction product.

CONCLUSION

We used biocatalysts to capture carbon dioxide in cost-effective and eco-friendly manner, in an effort to eliminate some of the drawbacks of conventional CCS technologies for carbon dioxide sequestration. Biocatalyst activities were evaluated by varying the reaction temperature and carbon dioxide concentration. The hydration rate of the biocatalysts was in the order of BCA>HDS>HCA>EPF. The activity was drastically reduced as the temperature was increased, due to unfolding of the protein structure; the optimum temperature was around 25 °C. Using a p-NPA, the reaction rates for BCA and HDS were determined as 230.7 $M^{-1}s^{-1}$ and 194.1 $M^{-1}s^{-1}$, respectively. Formation of $CaCO_3$, the final product of the carbon dioxide sequestration process, took about 5 seconds when the biocatalysts were used and 15 seconds when they were not used, indicating that the biocatalysts increased the $CaCO_3$ formation rate approximately three-fold. At present, the study of carbon dioxide sequestration using biocatalysts is essentially only fundamental research. However, carbon dioxide sequestration using biocatalysts is likely to be the most stable method for carbon dioxide capture and storage. In addition, $CaCO_3$ can be utilized as road pavement or paper coating materials.

ACKNOWLEDGEMENTS

This research was supported by a grant (CK3-101-1-0-0) from Carbon Dioxide Reduction & Sequestration Research Center, one of the 21st Century Frontier Programs funded by the Ministry of Education Science and Technology of the Korean government.

REFERENCES

1. NASA, Global Warming. *Goddard Space Flight Center*, **207711**, 286 (1998).
2. B. Metz, O. Davidson, H. de Coninck, M. Loos and L. Meyer, IPCC Special Report on Carbon Capture and Storage (2005).
3. V. Ramanathan, *Bulletin of the American Academy of Arts and Sciences*, 36 (2006).
4. OECD/IEA, Energy Technology Perspectives (2008).
5. A. K. Saha, A. K. Biswas and S. S. Bandyopadhyayc, *Sep. Purif. Technol.*, **15**, 101 (1999).
6. S. Bishnoi and G. T. Rochelle, *Chem. Eng. Sci.*, **55**, 5531 (2000).
7. Z. Ruihong, G. Fen, H. Yongqi and Z. Huanqi, *Micropor. Mesopor. Mater.*, **93**, 212 (2006).
8. Y. W. Park, I. H. Baek, S. D. Park, J. W. Lee and S. J. Park, *Korean Chem. Eng. Res.*, **45**, 573 (2007).
9. Y. D. Hwang, H. Y. Shin, H. H. Kwak and S. Y. Bae, *Korean Chem. Eng. Res.*, **44**, 588 (2006).
10. S. G. Bishnoi and T. Rochelle, *AIChE J.*, 48 (2002).
11. M. Aineto, A. Acosta, J. M. Rincon and M. Romero, *Fuel*, **85**, 2352 (2006).
12. B. P. Sullivan, K. Krist and H. E. Guard, *Electrical and electrocatalytic reactions of carbon dioxide*, Elsevier, New York (1993).
13. C. Ho and J. M. Strurevant, *J. Biol. Chem.*, **238**, 1 (1963).
14. R. C. Khalifah, *J. Biol. Chem.*, **246**, 2561 (1971).
15. M. Parissa, A. Koorosh and M. Nader, *Ind. Eng. Chem. Res.*, **46**, 921 (2007).
16. G. M. Bond, J. Stringer, D. K. Brandvold, A. F. Simsek, M. G. Medina and G. Egeland, *Energy Fuels*, **15**, 309 (2001).
17. S. W. Lee and C. S. Choi, *Cryst. Growth Des.*, **7**, 1463 (2007).
18. M. Vinoba, D. H. Kim, K. S. Lim, S. K. Jeong, S. W. Lee and M. Alagar, *Energy Fuels*, **25**, 438 (2011).
19. M. Parissa, A. Koorosh and M. Nader. *Ind. Eng. Chem. Res.*, **46**, 921 (2007).
20. A. Berman, L. Addadi and S. Weiner, *Nature*, **331**, 546 (1988).
21. B. Ray, *Cell. Mol. Life Sci.*, **33**, 1439 (1977).